

Synthesis, characterization and catalytic oxidation activity of zirconium doped K-OMS-2 type manganese oxide materials

R. Jothiramalingam, B. Viswanathan*, T.K. Varadarajan

Department of Chemistry, Indian Institute of Technology Madras, Chennai 600 036, India

Received 20 August 2005; received in revised form 24 January 2006; accepted 26 January 2006

Available online 20 March 2006

Abstract

Zirconium doped manganese oxide OMS-2 materials have been synthesized. The synthesized zirconium doped manganese oxide OMS-2 materials have been characterized by XRD, TGA, BET and TEM techniques. All the materials showed the OMS-2 type (cryptomelane) X-ray diffraction patterns and the thermal stability and BET surface area of zirconium doped OMS-2 materials are improved compared to the parent manganese oxide (K-OMS-2) material. Transmission electron micrographs showed the rod like needle shaped morphology and zirconia dispersion on fibrous morphology of as-synthesized zirconium doped manganese oxide OMS-2 materials. As synthesized zirconium incorporated OMS-2 catalysts have been tested for the liquid phase oxidation of side chain aromatic compounds (ethylbenzene and benzyl alcohol) and cyclohexanol. Zr-K-OMS-2 (Cry) has shown high conversion for ethylbenzene and benzyl alcohol, whereas Zr-K-OMS-2 (Bir) has shown high activity for the conversion of cyclohexanol and good selectivity towards the formation of cyclohexanone.

© 2006 Elsevier B.V. All rights reserved.

Keywords: Manganese oxide; OMS-2; Zirconium oxide; Birnessite; Benzyl alcohol; Ethyl benzene

1. Introduction

Octahedral molecular sieves (OMS) of manganese oxides are large in number and complex in character. The main origin of this material is manganese nodules (available in the deep-sea region) and some of the soil sediments. Naturally occurring manganese nodules contain large number of manganese oxide minerals [1]. The main phases present in the manganese nodules are birnessite type layer structured material and also cryptomelane, todorokite type tunneled structure manganese oxide phases. These materials play a valuable role in the field of catalysis for oxidation and oxidative dehydrogenation of specific organic substrates [2]. Birnessite type layered materials are used as cathode materials for lithium rechargeable batteries due to their two-dimensional layered structure [3] and also as precursors for the formation of todorokite type tunnel structured materials [4]. The main drawback associated with naturally occurring manganese oxide materials is that they are less crystalline and poor in homogeneity. Birnessite type layered manganese oxide material is com-

posed of alternately stacked sheets of MnO_6 octahedra linked through oxygen atoms and the water molecules occupy the interlayers. The interlayer spacing of this layered type manganese oxide material is nearly 7 Å (Fig. 1(a)). Recently, tunnel structured manganese oxide OMS materials such as cryptomelane (K-OMS-2) and todorokite (Mg-OMS-1) are exploited as catalysts for oxidation of volatile organic compounds [5].

Inside the tunnel structure of manganese oxide materials, potassium (cryptomelane) or magnesium (todorokite) ions are present as exchangeable cations. Potassium containing cryptomelane type manganese oxide OMS-2 material (Fig. 1(b)) consists of (2×2) matrices of tunnel structures with pore size of 4.6 Å and which has a general composition $\text{K}_{0.8-1.5}\text{Mn}_8\text{O}_{16}$ [1]. Fig. 1 shows the layer and tunnel structures of potassium birnessite and cryptomelane. Bulk zirconia is a well-known interesting and important material in the field of heterogeneous catalysis, as support for oxides [6] and metals [7]. Bulk zirconia and supported zirconia catalysts have been exploited as efficient catalysts for complete as well as partial oxidation reactions.

Recently, zirconium doped manganese oxide composite catalysts and Mn–Zr oxide catalysts prepared by the co-precipitation method have been investigated for catalytic oxidation of isopropyl alcohol and phenanthrene [8]. Zirconia-based catalysts

* Corresponding author. Tel.: +91 44 22578250; fax: +91 44 2350509.
E-mail address: bnathan@iitm.ac.in (B. Viswanathan).

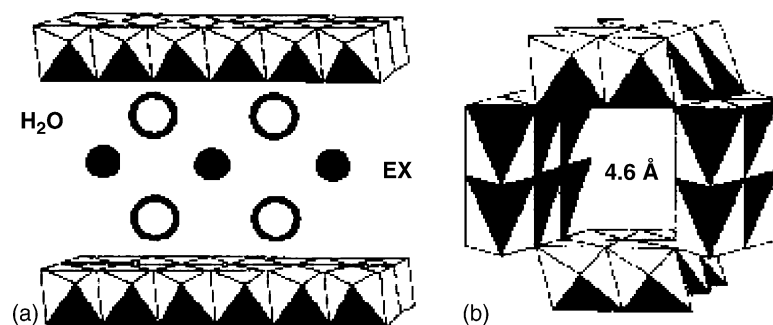


Fig. 1. (a) Potassium birnessite (Ex = K); (b) Cryptomelane type K-OMS-2 structure.

with different acid–base properties are synthesized and the relationship between isosynthesis activity and acid–base properties of the catalysts have also been studied [9]. Devassy et al. have recently reported the catalytic activity of different loadings of zirconia on 12-tungstophosphoric acid for the formation of linear alkylbenzenes [10]. Craciun et al. have studied the structure and redox properties of yttrium-incorporated zirconia supported on manganese oxide catalysts for CO and CH₄ oxidation [11].

In classical synthetic procedures, permanganate or dichromate is used as an oxidant for the oxidation of side chain aromatic compounds. Titanium substituted silicates usually catalyze ring hydroxylation of arenes and substitution of vanadium [12–14], tin [15–18] and chromium [19–21] into zeolite and aluminophosphate structures favors side chain oxidation. Most notably, chromium substituted aluminophosphate, Cr-APO-5, catalyzes the formation of ketones from alkyl arenes with TBHP (*tert*-butyl hydrogen peroxide) as oxidant in moderate yields with selectivity greater than 90% [21–23]. Role of lattice oxygen in manganese oxide OMS-2 catalyst in selective oxidation of benzyl alcohol in the presence of chemical oxidant has also been reported and they the mechanism of benzyl alcohol oxidation has been proposed based on kinetic and isotope labeling studies [24]. Incorporation of tetravalent zirconium into the ordered phase of tunneled manganese oxide OMS-2 type material can improve the thermal stability as well as alter the acidic–basic property of manganese oxide. It also provides catalytic activity for total oxidation of hazardous substances such as soot (a pollutant present in diesel engine waste gases) and removal of VOCs (volatile organic compounds). In the present study, the main objective is to synthesize the zirconium doped manganese oxide K-OMS-2 materials by the reflux method (pre-incorporation of zirconium) and by the impregnation method (post-incorporation of zirconium) from potassium birnessite and cryptomelane precursors. The reason for the present study is to found out which method of incorporation or doping (pre- or post-incorporation) of zirconium into K-OMS-2 type manganese oxide octahedral molecular sieve (OMS) material is effective for the oxidation of side chain aromatic substrates in the liquid phase. Another objective is to improve the thermal stability and surface area of as-synthesized zirconium doped manganese oxide OMS-2 materials comparable to the parent manganese oxide K-OMS-2. Thermal stability and improved surface area of as-prepared zirconium manganese oxide OMS-2 materials were probed by TGA and BET analysis. Catalytic activity of as-synthesized zir-

conium doped OMS-2 catalysts has also been tested for liquid phase oxidation of ethyl benzene, benzyl alcohol and cyclohexanol using a chemical oxidant *tert*-butyl hydroperoxide (TBHP). Zirconium doped manganese oxide OMS-2 materials prepared by post-incorporation showed good (48–62%) conversion for side chain compounds in the presence of the chemical oxidant.

2. Materials and methods

All the chemicals purchased from E-Merck and SRL (India) were reagent grade and the catalysts prepared were characterized by powder X-ray diffraction using a Philips Diffractometer (Philips Generator, Holland, Model PW 1140) provided with an online recorder. The diffraction patterns were recorded using Fe K α ($\lambda = 1.97 \text{ \AA}$) radiation at a scanning speed of $2^\circ/\text{min}$. Thermal stability and phase transitions were analyzed using a Perkin-Elmer TGA (Delta series TGA 7), at a heating rate of $10^\circ/\text{min}$. Transmission electron micrographs (TEM) were recorded using a Philips CM12/STEM- EDAX equipment. TEM sampling grids were prepared by placing $2 \mu\text{L}$ of the solution on a carbon-coated grid and the solution was evaporated at room temperature. Surface area and pore volume were obtained from N₂ adsorption–desorption isotherms using conventional BET and BJH methods. The calcined samples were outgassed under vacuum at 250°C . Isotherms were measured at liquid nitrogen temperature with a Carlo-Erba sorptometer (Model 1800). The products of the catalytic reactions were analyzed using gas chromatography (Nucon 5600, FID, SE 30 and OV 17 column).

3. Experimental

3.1. Zirconium incorporated manganese oxide OMS-2 catalysts prepared by pre-incorporation method

Zirconium containing manganese oxide OMS-2 material was synthesized by refluxing 30 mL of 1.75 M solution of manganese(II) sulphate and 95 mL of 0.4 M potassium permanganate solution (reaction mixture) in the presence of 6.8 mL of concentrated nitric acid (potassium permanganate and manganese sulphate reaction mixture in high acidic medium pH 2). The molar ratio between potassium permanganate and manganese sulphate was maintained at 0.72 and the molar ratio of Zr⁴⁺/Mn²⁺ at 0.20 for one sample (10.5 mL of 1.0 M zirconyl nitrate solution added to the reaction mixture solution) and at 0.25 for the second

sample (13.1 mL of 1.0 M zirconyl nitrate solution added to the reaction mixture solution). The above solution was refluxed for 24 h and the product was filtered, washed several times with distilled deionized water. The sample was dried at 383 K for overnight followed by calcination of the synthesized sample in air at 400 °C for catalytic study. The synthesized samples were designated as Zr-K-OMS-2 (0.20) and Zr-K-OMS-2 (0.25).

3.2. Zirconium incorporated manganese oxide OMS-2 catalysts prepared by post-incorporation method

Another two types of zirconium-modified manganese oxide OMS-2 catalysts were synthesized from potassium birnessite (precursor for Zr-K-OMS-2 (Bir)) and cryptomelane (precursor for Zr-K-OMS-2 (Cry)) type manganese oxide materials. Potassium birnessite type layer structure material is synthesized by oxidation of 0.5 M solution of manganese(II) acetate in strong alkaline medium. Hydrous $\text{Mn}(\text{OH})_2$ suspension was obtained by the dropwise addition of 70 mL of 5.0 M KOH solution to 40 mL of 0.5 M manganese(II) acetate. As synthesized manganese oxide suspension was then oxidized by 50 mL of 0.1 M potassium permanganate solution followed by ageing the precipitated suspension for 4–5 days. The molar ratio between MnO_4^- and Mn^{2+} was maintained at 0.36. After 4–5 days, the suspension was filtered, washed several times with double distilled water and dried at room temperature. As synthesized potassium birnessite (precursor for Zr-K-OMS-2 (Bir)) was then calcined for 5 h at 623 K to form the OMS-2 type tunnel structure. An appropriate amount of above synthesized manganese oxide OMS-2 (1.6 g) material mixed with 0.40 g of zirconyl nitrate was dissolved in methanol. The above mixture was stirred for 24 h, followed by evaporation of the solvent. As synthesized material was subjected to heat treatment at 673 K in air for 12 h, which resulted in the formation of zirconium containing manganese oxide OMS-2 catalyst, designated as Zr-K-OMS-2 (Bir).

Cryptomelane type parent manganese oxide OMS-2 material (precursor for Zr-K-OMS-2 (Cry)) [24] was synthesized by the reported procedure. 113 mL of 0.4 M solution of potassium permanganate was added to a 500 mL round bottom flask containing a mixture of manganese sulfate hydrate solution (33 mL of 1.75 M) and concentrated nitric acid (3.40 mL). As-synthesized manganese oxide OMS-2 material (K-OMS-2) was dried at 384 K for 24 h. Appropriate amount (0.40 g) of zirconyl nitrate was dissolved in methanol stirred with 1.60 g of as-synthesized K-OMS-2 material for 24 h, followed by evaporation of the solvent. As-synthesized material was then heat treated at 673 K for 5 h in air, designated as Zr-K-OMS-2 (Cry).

3.3. Oxidation of side chain aromatic compound and cyclohexanol

A mixture containing 100 mg catalyst, 15 mL of solvent (acetonitrile) and suitable amount of organic substrate were stirred in a round bottom flask equipped with a condenser. Then appropriate amount of the oxidant, TBHP (*tert*-butyl hydroperoxide), was added. The resulting mixture was then refluxed for 10 h at 338 K for ethylbenzene, benzyl alcohol or cyclohexanol. After

completion of the reaction time, the catalyst was removed by filtration and the filtrate was subjected to GC analysis.

4. Results and discussion

4.1. X-ray diffraction results

The X-ray diffraction patterns of the four types of zirconium modified tunneled manganese oxide OMS-2 catalysts such as Zr-K-OMS-2 (0.20), Zr-K-OMS-2 (0.25), Zr-K-OMS-2 (Bir) and Zr-K-OMS-2 (Cry) are shown in Fig. 2. The major *d*-spacing values match with the reported data of cryptomelane (OMS-2) (JCPDS: 34–168) and the corresponding (h k l) values are (1 0 1), (0 0 2), (3 0 1), (2 1 1), (3 1 0), (1 1 4) and (6 0 0) at 2θ values of 12.7, 18.0, 28.7, 37.4, 41.8, 50.0, 55.3. The crystalline phase of OMS-2 is not retained at higher loadings such as above 20 wt.% zirconia or above the molar ratio of $\text{Zr}^{4+}/\text{Mn}^{2+} = 0.25$.

4.2. Thermal stability of zirconium incorporated OMS-2 materials and morphology characterization

Fig. 3 shows the TGA (thermo gravimetric analysis) profile of parent K-OMS-2 material synthesized by the reflux method (without zirconium incorporation). Initial weight loss observed in the temperature range between 323 and 623 K is due to the removal of water molecules and loss of lattice oxygen present in the sample with a weight loss of 2.2%. The major and second weight loss observed (6.9%) in the temperature between 623 and 953 K, is due to the removal of more lattice oxygen from manganese oxide. This has resulted in manganese oxide OMS-2 phase transformed into lower oxidation state manganese oxide phase such as bixbyite [25]. The third weight loss (1.6%) observed in the temperature range between 953 and 1073 K is due to further decomposition of bixbyite phase into the lower oxidation state such as hausmanite [26]. TGA profiles of zirconium incorporated OMS-2 catalysts synthesized by

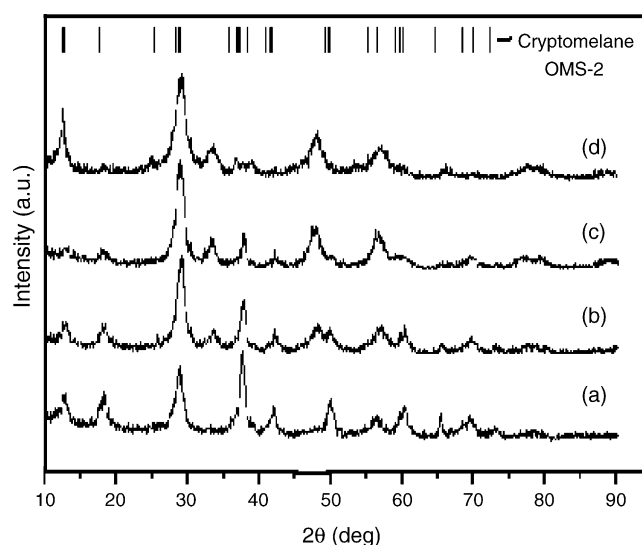


Fig. 2. XRD patterns of zirconium modified OMS-2 catalysts: (a) Zr-K-OMS-2 (0.20); (b) Zr-K-OMS-2 (0.25); (c) Zr-K-OMS-2 (Bir); (d) Zr-K-OMS-2 (Cry).

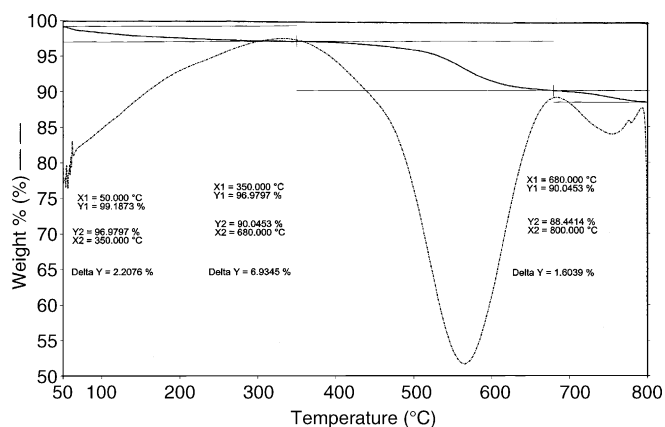


Fig. 3. TGA of parent manganese oxide OMS-2 material (K-OMS-2).

the impregnation method are shown in Fig. 4(a) [Zr-K-OMS-2 (Bir)] and Fig. 4(b) [Zr-K-OMS-2 (Cry)]. Zr-K-OMS-2 (Bir) catalyst shows the major weight loss in the temperature range of 573–1073 K (7.7%) and Zr-K-OMS-2 (Cry) in the range of 673–1073 K (5.0%), due to evolution of lattice oxygen and the decomposition of the OMS-2 phase into lower oxidation state manganese oxide phases such as bixbyite [25]. Zirconium incorporated manganese oxide Zr-K-OMS-2 (Cry) shows the major weight loss at higher temperatures 673–1073 K, whereas parent K-OMS-2 material (Fig. 3) shows the major weight loss in the temperature range between 623 and 953 K due to decomposition of OMS-2 phase into Mn_2O_3 .

BET surface areas and pore volumes of as-prepared parent K-OMS-2 material and zirconium incorporated OMS-2 materials are given in Table 1. The zirconium content present in

the samples was determined by TEM-EDAX analysis and also given in Table 1. Zirconium doped manganese oxide OMS-2 materials prepared by the post-incorporation method, [Zr-K-OMS-2 (Cry) and Zr-K-OMS-2 (Bir)], show higher zirconium content than zirconium doped manganese oxide OMS-2 materials prepared by the reflux method. BET surface area values of as-synthesized zirconium incorporated OMS-2 catalysts are found to be high (50–85 m^2/g) compared to the conventionally synthesized Mn–Zr composite oxide materials [8,27].

Surface density of zirconia on manganese oxide OMS-2 phase has also been calculated by the reported method [10], and is given in Table 1. Zirconium doped manganese oxide OMS-2 materials prepared by the post-incorporation method [Zr-K-OMS-2 (Cry) and Zr-K-OMS-2 (Bir)] show the higher surface density of zirconia on the manganese oxide OMS-2 phase than manganese oxide OMS-2 materials prepared by the pre-incorporation method. Pore volumes of all zirconium doped manganese oxide OMS-2 materials (Table 1) are similar in the range of 0.21–0.22 cm^3/cc . TEM micrographs of zirconium incorporated OMS-2 catalyst [Zr-K-OMS-2 (0.25)] are shown in Fig. 5(a) and (b) (zirconium containing OMS-2 material prepared by the pre-incorporation method). TEM micrographs of zirconium incorporated OMS-2 catalysts synthesized by the impregnation method shown in Fig. 5(c) and (d) [Zr-K-OMS-2 (Bir)] and Fig. 5(e) and (f) [Zr-K-OMS-2 (Cry)]. Zirconium incorporated OMS-2 catalyst prepared by the pre-incorporation method shows a rod like morphology with length of 550 nm and diameter of 110 nm as well as agglomerated particle morphology of particle size of 100–105 nm (Fig. 5(a) and (b)).

Zr-K-OMS-2 (Bir) catalyst showed zirconia particles finely dispersed on the fibrous morphology of manganese oxide

Table 1
Physico-chemical parameters of zirconium incorporated OMS-2 catalysts

Catalysts	Surface area (m^2/g)	Pore volume (cm^3/g)	Zirconium content (at.%)	Surface density (Zr) (nm^2)
Zr-K-OMS-2 (0.20)	62	0.208	2.8	2.98
Zr-K-OMS-2 (0.25)	81	0.207	3.6	2.94
Zr-K-OMS-2 (Bir)	68	0.293	6.2	6.09
Zr-K-OMS-2 (Cry)	51	0.210	4.7	6.03
K-OMS-2	45	0.213	–	–

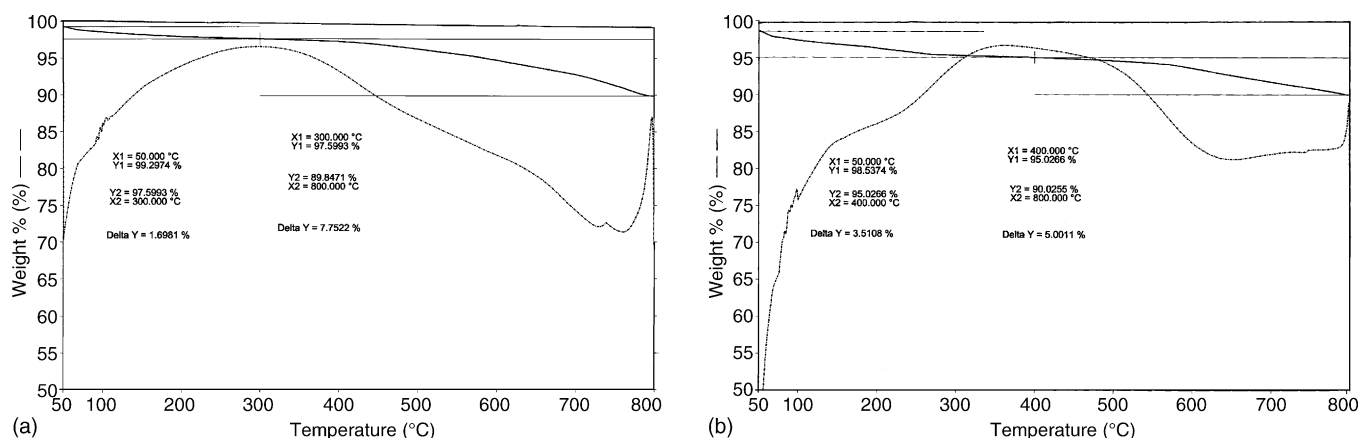


Fig. 4. TGA of zirconium incorporated OMS-2 catalysts: (a) Zr-K-OMS-2 (Bir); (b) Zr-K-OMS-2 (Cry).

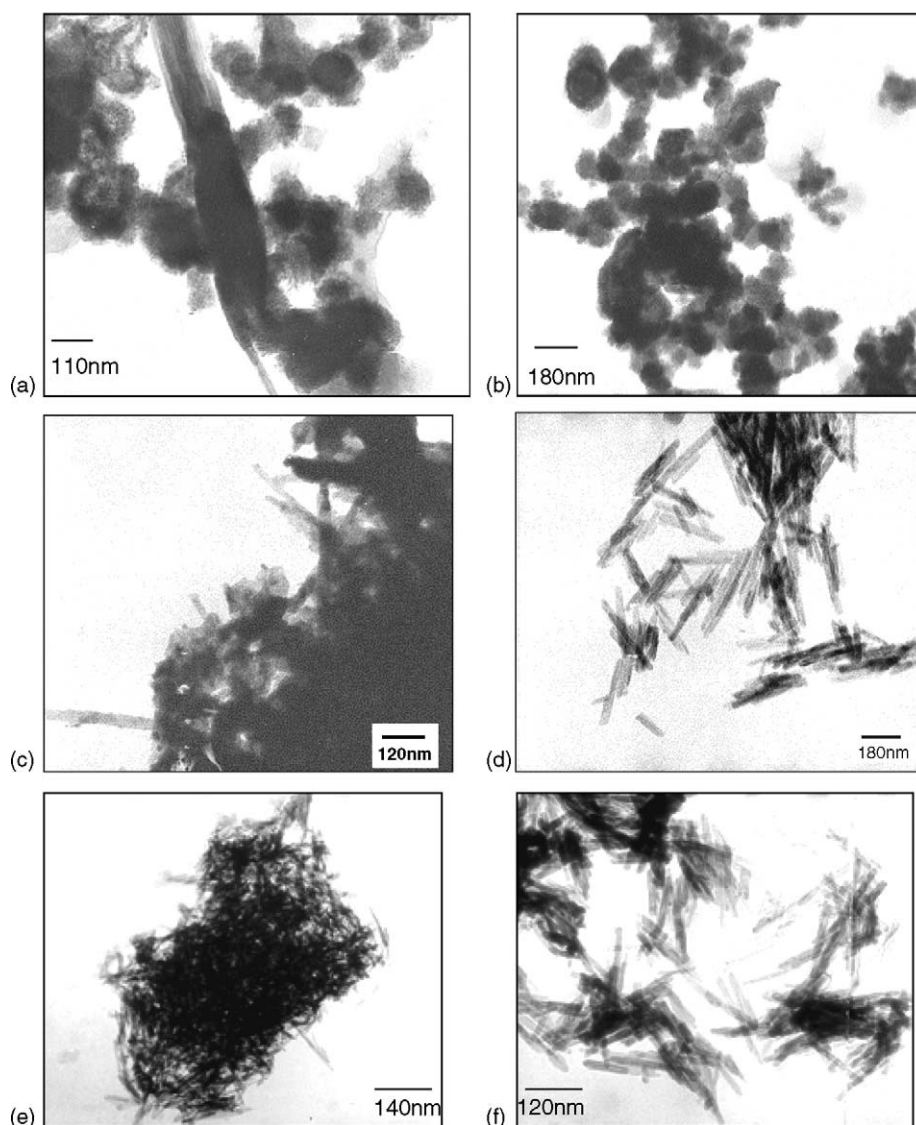


Fig. 5. (a and b) TEM pictures of Zr-K-OMS-2 (0.25); (c and d) TEM pictures of Zr-K-OMS-2 (Bir); (e and f) TEM pictures of Zr-K-OMS-2 (Cry).

OMS-2 material (Fig. 5(c) and (d)). Zr-K-OMS-2 (Cry) catalyst shows densely aggregated zirconia particle dispersion on fibrous or needle shaped morphology of manganese oxide OMS-2 material (Fig. 5(e) and (f)).

4.3. Catalytic activity of zirconium incorporated OMS-2 materials

Oxidation of side chain aromatic and arene compounds into their corresponding ketones are industrially important processes [28–30]. Bennur et al. have recently reported the oxidation of ethylbenzene on macrocyclic (tri- and tetra-) copper complex encapsulated zeolite-Y catalysts using TBHP dissolved in isooctane as the chemical oxidant [29]. In the present study, as-synthesized zirconium modified tunnel structured manganese oxide OMS-2 catalysts are tested for the liquid phase oxidation of ethylbenzene and benzyl alcohol using TBHP as the oxidant. The conversion of ethylbenzene on zirconium incorporated manganese oxide OMS-2 catalysts with different amounts

of TBHP is given in Tables 2 and 3. Benzyl alcohol conversion on zirconium incorporated manganese oxide OMS-2 catalysts is given in Table 4. Table 5 shows the liquid phase oxidation of cyclohexanol on zirconium incorporated OMS-2 catalysts. Zr-K-OMS-2 (Cry) catalyst shows a slightly higher conversion with 100% selectivity towards benzaldehyde. All zirconium incorporated manganese oxide OMS-2 catalysts show moderate ethyl

Table 2
Oxidation of ethyl benzene with TBHP in CH₃CN

Catalysts	Conversion (%)	Selectivity (%) (acetophenone)
Zr-K-OMS-2 (0.20)	26.2	98
Zr-K-OMS-2 (0.25)	20.4	98
Zr-K-OMS-2 (Bir)	34.8	98
Zr-K-OMS-2 (Cry)	37.4	98
K-OMS-2	10.5	98

Reaction condition: solvent (acetonitrile)=15 mL, substrate (ethyl benzene)=94 mmol, TBHP=70 mmol, weight of the catalyst=100 mg, $T=338$ K, duration=10 h.

Table 3
Oxidation of ethyl benzene with TBHP in CH₃CN

Catalysts	Conversion (%)	Selectivity (%) (acetophenone)
Zr-K-OMS-2 (0.20)	31.2	98
Zr-K-OMS-2 (0.25)	25.4	98
Zr-K-OMS-2 (Bir)	36.6	98
Zr-K-OMS-2 (Cry)	62.4	98
K-OMS-2	19.0	98

Reaction condition: solvent (acetonitrile) = 15 mL, substrate (ethyl benzene) = 94 mmol, TBHP = 140 mmol, weight of the catalyst = 100 mg, $T = 338$ K, duration = 10 h.

Table 4
Oxidation of benzyl alcohol with TBHP in CH₃CN

Catalysts	Conversion (%)	Selectivity (%) (benzaldehyde)
Zr-K-OMS-2 (0.20)	24.2	100
Zr-K-OMS-2 (0.25)	18.4	100
Zr-K-OMS-2 (Bir)	39.7	100
Zr-K-OMS-2 (Cry)	48.4	100
K-OMS-2	14.0	100

Reaction condition: solvent (acetonitrile) = 15 mL, substrate (benzyl alcohol) = 360 mmol, TBHP = 140 mmol, weight of the catalyst = 150 mg, $T = 338$ K, duration = 10 h.

benzene conversion with good selectivity towards acetophenone formation (refer Tables 2 and 3).

All zirconium incorporated manganese oxide OMS-2 catalysts show 26–62% ethylbenzene conversion with 98% selectivity towards acetophenone formation (Tables 2 and 3). The zirconium incorporated manganese oxide catalyst [Zr-K-OMS-2 (Cry)] shows 62% conversion of ethylbenzene, (Table 3). Benzyl alcohol and cyclohexanol conversion on zirconium incorporated manganese oxide OMS-2 catalysts are given in Tables 4 and 5. The Zr-K-OMS-2 (Cry) catalyst shows 48.4% conversion for benzyl alcohol oxidation with 100% selectivity towards benzaldehyde formation. Ethylbenzene and benzyl alcohol conversion for the same amount (140 mmol) of TBHP on zirconium incorporated OMS-2 catalysts shows good selectivity towards the specific product formation (acetophenone and benzaldehyde). Zr-K-OMS-2 (Cry) catalyst shows higher conversion of ethylbenzene and benzyl alcohol compared to other catalysts, whereas Zr-K-OMS-2 (Bir) catalyst shows only 18.4% conversion of cyclohexanol (Table 5) and 100% selectivity towards cyclohexanone formation.

Table 5
Oxidation of cyclohexanol with TBHP in CH₃CN

Catalysts	Conversion (%)	Selectivity (%) (cyclohexanone)
Zr-K-OMS-2 (0.20)	13.3	100
Zr-K-OMS-2 (0.25)	14.5	100
Zr-K-OMS-2 (Bir)	18.4	100
Zr-K-OMS-2 (Cry)	16.2	100
K-OMS-2	9.8	100

Reaction condition: solvent (acetonitrile) = 15 mL, substrate (cyclohexanol) = 410 mmol, TBHP = 70 mmol, weight of the catalyst = 150 mg, $T = 338$ K, $t = 10$ h.

The substrates chosen for catalytic oxidation by zirconium modified OMS-2 catalysts affect the oxidation process. Substrates, ethylbenzene and benzyl alcohol are aromatic cyclic compounds, therefore carbocation formation in the rate-determining step is stabilized by resonance delocalization in the case of ethylbenzene and benzyl alcohol, and hence these two substrates show high conversion on zirconium modified OMS-2 catalysts compared to cyclohexanol oxidation on the same catalysts. Whereas Zr-K-OMS-2 (Bir) shows high conversion of 18.4% towards cyclohexanone formation compared to Zr-K-OMS-2 (Cry) catalysts, because of the presence of weak basic sites on Zr-K-OMS-2 (Bir) material, which facilitate the rate-determining step by stabilizing the intermediate carbocation. This results in maximum cyclohexanol conversion towards cyclohexanone formation.

Ethylbenzene and benzyl alcohol oxidation reaction has also been carried out on parent K-OMS-2 under the same reaction conditions in the presence of TBHP. Parent K-OMS-2 material showed only 19% conversion of ethylbenzene and 14% conversion of benzyl alcohol oxidation. The zirconium incorporation in OMS-2 manganese oxide material facilitates the partial oxidation reactions in the presence of oxidant TBHP.

Bennur et al. have recently reported the oxidation of ethylbenzene on macrocyclic (tri- and tetra-) copper complex encapsulated zeolite-Y catalysts using TBHP dissolved in isooctane as the chemical oxidant [29]. One of the main advantages of as synthesized zirconium incorporated manganese oxide OMS-2 catalysts is the simple synthetic route to the preparation of catalyst compared to other routes such as sol-gel and co-precipitation methods.

5. Conclusions

Zirconium incorporated manganese oxide OMS-2 catalysts prepared by the reflux method and by the impregnation method instead of composite MnO_x-ZrO₂ catalysts prepared by the co-precipitation method prepared and as-synthesized zirconium incorporated K-OMS-2 materials showed higher surface area values compared to parent K-OMS-2. The morphology of as-synthesized zirconium incorporated OMS-2 materials depends upon the preparation method. Rod like particle morphology is obtained for material synthesized by the reflux method [Zr-K-OMS-2 (0.25)], whereas catalysts [Zr-K-OMS-2 (Cry) and Zr-K-OMS-2 (Bir)] prepared by the impregnation method showed non-uniform dispersion of zirconia particles on fibrous morphology of manganese oxide phase. The synthesized zirconium incorporated catalysts are tested for the partial oxidation of side chain aromatic compounds and alcohol. The manganese oxide OMS-2 catalyst Zr-K-OMS-2 (Cry) synthesized by the impregnation method showed efficient conversion for oxidation of ethylbenzene, benzyl alcohol and Zr-K-OMS-2 (Bir) catalyst showed fairly good conversion for cyclohexanol oxidation towards cyclohexanone formation. Zirconium doped OMS-2 type manganese oxide catalysts with improved surface area, may function as potential catalysts for complete oxidation of hazardous volatile organic compounds (VOCs).

References

- [1] J.E. Post, Proc. Natl. Acad. Sci. U.S.A. 96 (1999) 3447.
- [2] R. Ghosh, Y.C. Son, V.D. Makwana, S.L. Suib, J. Catal. 224 (2004) 288.
- [3] S. Bech, J.P. Pereiga-Ramos, N. Baffier, Electrochem. Acta 38 (1993) 1695.
- [4] X. Chen, Y.F. Shen, S.L. Suib, C.L. O'young, Chem. Mater. 14 (2002) 940.
- [5] J. Luo, Q. Zhang, A. Huang, S.L. Suib, Micropor. Mesopor. Mater. 35/36 (2000) 209.
- [6] M. Murakami, K. Inomata, T. Mori, K. Uli, G. Suzuki, P. Poncelet, P.A. Grange, Jacobs (Eds.), Preparation of Catalysts, vol. III, Elsevier, Amsterdam, 1998, p. 531.
- [7] H. Fuji, N. Mizumo, M. Misono, Chem. Lett. (1987) 2147.
- [8] E.F. Lopez, V.S. Escibino, C. Resini, J.M. Gallorad-Amores, G. Busca, Appl. Catal. B: Environ. 29 (2001) 251.
- [9] Z.T. Feng, W.S. Postula, A. Akgerman, R.G. Anthony, Ind. Eng. Chem. Res. 34 (1995) 78.
- [10] B.M. Devassy, F. Lefebvre, S.B. Halligudi, J. Catal. 231 (2005) 1.
- [11] R. Craciun, B. Nentwick, K. Hadjiivanov, H. Knozinger, Appl. Catal. A: Gen. 243 (2003) 67.
- [12] P. Kumar, R. Kumar, B. Pandey, Synlett (1995) 289.
- [13] K.R. Reddy, A.V. Ramaswamy, P. Ratnasamy, J. Catal. 143 (1993) 275.
- [14] T. Sen, M. Chatterjee, S. Sivasanker, J. Chem. Soc. Chem. Commun. (1995) 207.
- [15] A. Bhaumik, M.K. Dongare, R. Kumar, Micropor. Mater. 5 (1995) 173.
- [16] P. Ratnasamy, R. Kumar, Stud. Surf. Sci. Catal. 97 (1995) 501.
- [17] R. Vetrivel, P.R. Hari Prasad Rao, A.V. Ramaswamy, Stud. Surf. Sci. Catal. 83 (1995) 109.
- [18] T. Selvam, A.P. Singh, J. Chem. Soc. Chem. Commun. (1995) 883.
- [19] K.R. Reddy, A.V. Ramaswamy, P. Ratnasamy, J. Chem. Soc. Chem. Commun. (1992) 1613.
- [20] N.K. Mal, V. Ramaswamy, S. Ganapathy, A.V. Ramaswamy, Appl. Catal. 125 (1995) 233.
- [21] J.D. Chen, R.A. Sheldon, J. Catal. 153 (1995) 1.
- [22] J.D. Chen, H.E.B. Lempers, R.A. Sheldon, J. Chem. Soc. Faraday Trans. 92 (1996) 1807.
- [23] J.D. Chen, M.J. Haanepen, J.H.C. van Hooff, R.A. Sheldon, Stud. Surf. Sci. Catal. 84 (1994) 973.
- [24] V.D. Makwana, Y.C. Son, A.R. Howell, S.L. Suib, J. Catal. 210 (2002) 46.
- [25] M.I. Zaki, A.K.H. Nohman, G.A.M. Hussein, Y.E. Nashed, Colloids Surf. A 99 (1995) 247.
- [26] A.K.H. Nohman, H.M. Ismail, G.A.M. Hussein, J. Anal. Appl. Pyrol. 34 (1995) 265.
- [27] K. Eguchi, M. Watabe, S. Ogata, H. Arai, Bull. Chem. Soc. Jpn. 68 (1995) 1739.
- [28] J.F. Pan, K. Chen, J. Mol. Catal. A: Gen. 176 (2001) 19.
- [29] T.H. Bennur, D. Srinivas, S. Sivasanker, J. Mol. Catal. A 207 (2004) 163.
- [30] M. Rogovin, R. Neumann, J. Mol. Catal. A: Gen. 138 (1999) 315.